Adsorption of Molybdate Monomers and Polymers on Titania with a Multisite Approach

K. Bourikas,† T. Hiemstra,* and W. H. Van Riemsdijk

Department of Environmental Sciences, Wageningen University, P.O. Box 8005, NL 6700 EC Wageningen, The Netherlands

Received: June 22, 2000; In Final Form: November 8, 2000

Adsorption of polymers on mineral surfaces is of great interest. A representative important system is the molybdenum supported titania, used in catalysis. The well-known chemistry of molybdate polymers in aqueous solutions allows a detailed study of the contribution of these polymers to the Mo adsorption on titanium oxide surface. A large range of Mo concentrations was covered: from low levels where only Mo monomers are present to high levels where extensive polymerization takes place. Data from different techniques, like potentiometric titrations, proton−ion titrations, and adsorption edges, were used for the description of the interface "molybdate solution/titania surface". All the data could be modeled very well using the recently introduced CD−MUSIC approach. The charge of the surface complexes is spatially distributed in the interface. MoO_4^{2-} monomers adsorb over the entire pH range forming inner sphere complexes, which are characterized by two types of structure, i.e., bidentate and monodentate. Below pH 5.5 and high total molybdate concentrations the heptamolybdate polyanion $Mo_7O_{23}(OH)^{5-}$ is also adsorbed, forming an outer sphere complex. Due to its relatively large size, it covers a significant number of surface groups.

Introduction

Anion and cation adsorption at the solid/solution interface of metal (hydr)oxides is an important phenomenon in many fields of chemistry. It is of great interest among soil chemists and geochemists studying the natural environment, among colloid chemists studying colloidal systems and many scientists involved in chemical engineering. Over the past decades, there also have been an increasing number of related studies in catalysis.

A significant part of heterogeneous catalysis is dedicated to the supported catalysts.[1,2] These materials are usually prepared by impregnating the support—which is usually a metal oxide—in an electrolytic solution containing the active element to be deposited. Filtration, drying, and calcination follow. The impregnation step, where adsorption of the active element on the oxide surface takes place, is often critical because it can significantly determine the properties of the final catalyst. Depending on the impregnating conditions (pH, concentration, ionic strength, etc.), several ionic species of the element may occur in the suspension. For several elements, high concentrations result in the formation of polymers in the suspension. The polymers may be adsorbed on the support surface. Elucidation of the factors determining the adsorption process of the polymers will allow the tailoring of the preparation of the catalyst by regulating the impregnation parameters.

Various models have been used to describe adsorption data.[3−12] They are tested on the basis of the possibility of describing these data and predicting results. Most popular are the surface complexation models including an electrostatic double layer option. For a limited set of data many different models give similar results.[13] As a result of this, there is an increasing demand for new experiments and new information from other related fields that could help in the direction of discriminating among all these models. Particularly, the use of in situ spectroscopic techniques, revealing the physical chemical structure of the surface species, has provided useful information for the models.[14−22]

In most commonly used surface complexation models it is difficult to take advantage of structural details since species are treated as point charges. This difficulty has been overcome with the CD−MUSIC model (charge distribution−multisite complexation).[23] This model emphasizes the importance of the surface structure and the structure of adsorbed species. Surface complexes are not treated as point charges but are considered to have a spatial distribution of charge in the interfacial region. The model has been applied in several oxy-anion systems related to adsorption of monomers.[23−28] In most cases, its predictions are consistent with physically realistic surface complexes found by spectroscopy.

In this paper, we will apply this model to describe the adsorption of molybdenum on the surface of titanium oxide. Our approach is based on a large range of adsorption data, from very low to high adsorption levels, where polymeric molybdate species are formed. This system was selected for two important reasons: The first is its great importance and use in the heterogeneous catalysis. The second is the simple and well-known chemistry of the aqueous molybdate solution, even at high concentrations where polymers are found. The study of this system may show the way that could be followed for studying similar important systems, where polymers are included in an adsorption process.

Studies dealing with supported molybdate catalysts prepared by the adsorption method are not abundant in the literature.[29−33] Most of these studies focused on the structure of the adsorbed molybdates after calcination of the samples. Although this kind of characterization can give useful information about the properties of the final catalyst, it cannot reveal the adsorption

* To whom correspondence should be addressed. E-mail: tjisse.hiemstra@bodsch.benp.wag-ur.nl.

† On leave from the Department of Chemistry, University of Patras, and the Institute of Chemical Engineering and High-Temperature Chemical Processes, ICE/HT-FORTH, P.O. Box 1414, GR-26500 Patras, Greece.

10.1021/jp002267q CCC: $20.00
Published on Web 03/03/2001

mechanism of the molybdates on the titania surface. The first detailed study to this direction was done by the group of Lycourghiotis.[34,35] Using an approach[11] based on the widely known homogeneous two pK − triple layer model, they described a wide range of adsorption data quite well. However, the final surface speciation remains uncertain due to a number of simplifying assumptions. Particularly, the treatment of the adsorbed species, even the large polymers, as point charges and the nonrealistic picture of a homogeneous surface as well as the relatively large amount of the adjustable parameters are a part of that.

In this paper, by applying the CD−MUSIC model and using the experience of the previous approach, we will try to overcome these limitations, improving our understanding of the nature and the structure of the adsorbed molybdates on titania. To separate clearly between monomer and polymer adsorption, we will first study the monomer adsorption extensively. This can be done at low levels of molybdate loading. At these conditions, a very powerful tool for characterizing accurately the adsorption is the determination of the proton−molybdate stoichiometry at constant pH. This will be done my measuring the proton coadsorption as a function of the molybdate adsorption. It provides direct information about the pH dependency of the adsorption.[36,37] It is also useful in the interpretation of the binding structure of the adsorbed molybdate.[38] Particularly, a sensitive determination of the charge distribution of the adsorbed species can be achieved.

After characterization of the monomer adsorption, the model will be applied to conditions where polymeric molybdate species are adsorbed.

Materials and Methods

Synthesis and Characterization. All chemicals (Merck p.a.) were stored in plastic bottles, and all experiments were done in plastic vessels to avoid silica contamination. The temperature was kept constant at 25 °C, and the ionic strength was equal to 0.1 M. Ultrapure boiled water was used to prepare all solutions.

For the proton−molybdate titrations and the adsorption edges at low levels, pure anatase was used, prepared by hydrolysis of titanium isopropoxide (Alfa).[39] The specific surface area (SSA), determined with BET measurements, is 40 $m^2\ g^{-1}$. Sodium molybdate and sodium nitrate stock solutions were prepared from the corresponding crystalline reagents.

For the edges at high adsorption levels, commercially available titania (Degussa P25) was used, with a specific surface area of 50 $m^2\ g^{-1}$. The patchwise structure of the surface consists mainly of anatase.[40−42] Ammonium heptamolybdate and ammonium nitrate stock solutions were prepared from the corresponding crystalline reagents.

The choice of the commercial titania as well as of the ammonium heptamolybdate and nitrate was for reasons of comparing results with previously reported data on the same system.[34] Moreover, this titania is the most commonly used in the preparation of titania supported catalysts. The use of ammonium reagents is preferred in catalysis because of the easy removal of ammonium in the heating process. In the case of low adsorption levels, we used sodium molybdate and nitrate instead of ammonium heptamolybdate and nitrate in order to avoid possible proton release due to transformation of NH_4^+ to NH_3 at high-pH values. This could influence the proton−molybdate coadsorption stoichiometry.

Mo Speciation in Solution. Ammonium heptamolybdate solution (0.016 25 M) was added to 50 mL of 0.100 M NH_4NO_3 solution at 25.0 °C in a vessel purged with moist N_2 gas, and the pH was registered. The experiment was repeated with 0.001 625 M $(NH_4)_6Mo_7O_{24}$ in 0.090 M NH_4NO_3 added to 49 mL of 0.100 M NH_4NO_3. The 0.100 M NH_4NO_3 solution was slightly acidic, having an initial pH of the 5.32, probably due to removal of very small amounts of NH_3(g). In titration experiments 0.375 or 3.75 mL of 0.016 25 M $(NH_4)_6Mo_7O_{24}$ was added to 75 mL of 0.100 M NH_4NO_3 and titrated with 0.0976 M NaOH. A N_2 atmosphere was kept above this solution (25.0 °C).

Proton−Ion Titrations at Constant pH. Vessels containing approximately 50 mL of 20−60 g L^{-1} titania were purged with moist nitrogen gas at pH < 6 for 1 day to remove CO_2 (I = 0.1 M). Next, the pH of the suspension reached the appropriate pH of the experiment with the addition of a small amount of acid (HNO_3) or base (NaOH). The suspension was kept (pH-stat) at this pH for about 1 h to reach equilibrium. Then, it was titrated with a 0.01 M sodium molybdate solution. During each addition of 0.2−0.5 mL of Na_2MoO_4 the pH was kept constant by titration with standardized 0.01 M HNO_3. A reaction time of about 20 min was enough for the system to reach equilibrium. Under the experimental conditions the solution Mo concentration was negligible compared to the adsorbed one, giving practically almost 100% adsorption (except pH = 8). This was certified by taking a filtrated sample for analysis with ICP-MS after the end of each titration. The proton coadsorption is calculated from the difference between the number of protons added to the suspension and the very small change in the number of protons in the solution. If almost no Mo remains in the solution, the Mo adsorption follows directly from the added amount of Mo.[38]

Adsorption Edges. Adsorption experiments were done at different initial Mo concentrations (10^{-6}, 10^{-5}, 10^{-4}, 10^{-3}, 10^{-2}, and 2×10^{-2} M). They were performed in individual plastic tubes (20 mL), with fixed amounts of titania, electrolyte, molybdate, and different amounts of acid or base, to give adsorption edges. To avoid contact with CO_2 at high-pH values, a CO_2 free titania suspension was mixed with the solution in the tubes, under nitrogen atmosphere. The tubes were closed immediately and then equilibrated for 24 h by end-over-end rotation. After measuring the final pH, the tubes were centrifuged and samples of the supernatants were taken for analysis with ICP-MS. The amount of the adsorbed molybdate was calculated from the difference between the total initial Mo concentration and that of the supernatant.

Model Calculations. Calculations were carried out with ECOSAT,[43] a computer code for the calculation of chemical equilibria. The solution and the surface equilibria used are presented in the Appendix.

Model Description

Multisite Complexation (MUSIC). Metal oxides are characterized by the presence of different types of surface groups. The multisite complexation model takes into account this surface heterogeneity. Variation in types of surface oxygens is due to a different number of coordinating metal ions. The charge on these surface oxygens can be found by applying the Pauling bond valence concept.[44] In this concept, the charge of the central metal ion is distributed over the coordinating oxygens.

The structure of titanium oxide consists of Ti^{4+} filled oxygen octahedra. The oxygens in the bulk of the solid are triply coordinated (Ti_3O^0), receiving from each Ti^{4+} a bond valence of 2/3 (each Ti^{4+} ion distributes its charge over six surrounding oxygens). The surface oxygens may be singly, doubly, and triply coordinated, depending on the number of the coordinating Ti^{4+} ions. Their coordination is lower than those of the bulk because

of some missing bonds. The binding of one or two protons can compensate the missing charge. In the case of singly coordinated groups, three species can be defined: $TiO^{-4/3}$, $TiOH^{-1/3}$, and $TiOH_2^{+2/3}$. It has been shown[45−47] that the constants of two consecutive protonation steps differ very strongly. For the singly coordinated Ti groups this implies that only the second protonation step is of relevance for the charging behavior.

On the basis of the above concepts, the charging behavior of the titania surface can be described by the following protonation reactions of singly and doubly coordinated groups:

$$TiOH^{-1/3} + H^+ \overset{K_{H1}}{\longleftrightarrow} TiOH_2^{+2/3} \quad (1)$$

$$Ti_2O^{-2/3} + H^+ \overset{K_{H2}}{\longleftrightarrow} Ti_2OH^{+1/3} \quad (2)$$

Protonation of the uncharged triply coordinated groups, Ti_3O^0, is not possible in the normal pH range. Therefore, these groups are considered inert in normal conditions. An extended description of the MUSIC model can be found elsewhere.[45,46]

CD Approach. An extension of the above-mentioned bond valence concept to surface complexation forms the basis of the CD model.[23] The charge of surface complexes is distributed over two electrostatic planes. A schematic representation of this idea is given in Figure 1. The charge of the surface groups is located at the surface plane (0-plane). Adsorbed ions are distinguished in inner sphere complexes and outer sphere complexes.

The inner sphere complexes are assumed to have a spatial distribution of the charge. Part of their charge is attributed to the surface (since not all ligands of the adsorbed complex are common with the surface) and the remaining of the part is attributed to the first plane (1-plane), at a certain distance from the surface. This means that a fraction f of the charge of the central ion (z_{Me}) of the complex is placed at the 0-plane and the remaining fraction ($1 - f$) is placed at the 1-plane. The change in charge in the 0-plane (Δz_0), due to the ion adsorption, is determined by the fraction of the charge of the central ion placed on the surface (fz_{Me}) plus the change of the charge due to the change in the number of protons (Δn_H) on the surface ligands involved in the surface reaction. Thus, Δz_0 can be defined as

$$\Delta z_0 = \Delta n_H z_H + f z_{Me} \quad (3)$$

where z_H is the valence of the proton. The Δn_H depends on the number of common ligands and the change in the state of protonation of these ligands. Its value may be positive, zero, or negative. The change in charge in the 1-plane (Δz_1) is determined by the fraction of the charge of the central ion placed in the 1-plane, $(1 - f)z_{Me}$, plus the sum of the charges of the solution oriented ligands ($\sum m_j z_j$):

$$\Delta z_1 = (1 - f)z_{Me} + \sum_j m_j z_j \quad (4)$$

where m_j and z_j are respectively the number and the charge of these ligands. In case of an ion surrounded by four ligands, as presented in Figure 1, an equal distribution of the charge of the central ion gives $f = 0.25$ for a monodentate complex (since one of its four ligands is common with the surface) and $f = 0.5$ for a bidentate complex (since two of its four ligands are common with the surface). The fraction f is also called the CD value.

It should be mentioned here that, as has been suggested,[48−50] only the singly coordinated surface groups are reactive for inner sphere complex formation of the anions. Considering an inner sphere molybdate complex binding to a singly, doubly, or triply coordinated group, we can calculate the sum of the bond valences on surface oxygen (Ti−O−Mo, Ti_2–O−Mo, Ti_3–O−Mo). Assuming a Pauling bond valence for a Mo−O bond of 1.5 vu (valence unit) and for a Ti−O bond of 2/3, this sum is equal to 0.17, 0.83, and 1.5 vu, respectively. According to literature,[51] only a neutral or almost neutral sum of bond valences is possible, implying that only the singly coordinated surface oxygens are reactive for an inner sphere molybdate complexation.

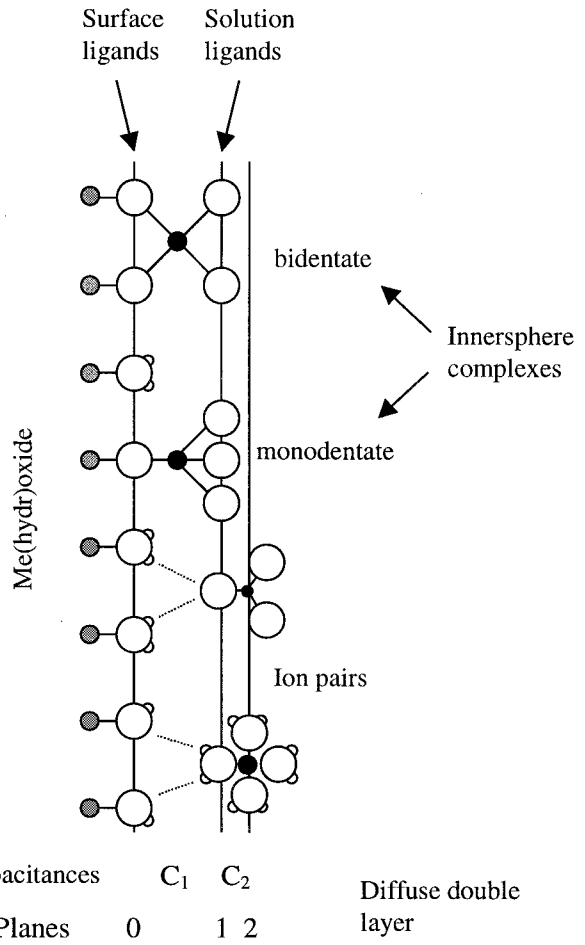

Figure 1. Schematic representation of the metal (hydr)oxide/solution interface (TP). Surface groups are coordinated with metal ions of the solid phase, and the corresponding charge is located in an electrostatic plane (0-plane). The surface groups may form inner sphere complexes with adsorbed ions. The surface-oriented ligands of inner sphere complexes are also located in the surface plane (0-plane). A bidentate surface complex has two common ligands, a monodentate surface complex one. The solution directed ligands of the inner sphere complexes are located in the inner plane of the compact part of the double layer (1-plane). The charge of the central ion of the inner sphere complexes is distributed over both electrostatic planes. Pair forming ions are treated as point charges and placed in the outer plane (2-plane). The space between a set of electrostatic planes is characterized by a capacitance.

The outer sphere complexes of electrolyte ions are placed at a position determined by the minimum distance of approach of hydrated ions to the (hydr)oxide surface. They form ion pairs with the surface groups without having common ligands with them. They are located in the outer plane (see Figure 1) and treated as point charges in the CD model, like the counterions of the diffuse part of the double layer (DDL).

In the case of an absence of surface complexation, the model becomes identical with the basic Stern layer model, and the compact part of the double layer is characterized by the well-known Stern capacitance (C). Inner sphere surface complexes divide the Stern layer in two parts, the inner layer with C_1 capacitance and the outer one with C_2 capacitance. These are related to the overall Stern layer capacitance according to the following:

$$\frac{1}{C} = \frac{1}{C_1} + \frac{1}{C_2} \tag{5}$$

The above-presented electrostatic approach is known as the three plane model (TP).[13,23] The TP differs from the widely used triple layer model (TLM) on the following parts:

(i) In the TLM, the adsorbed species are considered as point charges usually located at the surface plane. In the CD−MUSIC model, the adsorbed species are assumed to have a spatial distribution of their charge over two electrostatic planes (0 and 1 planes).

(ii) In the TLM ion pair formation is placed in the 1-plane, while in the TP model ion pairs are located in the 2-plane.

(iii) The capacitance of the outer layer in the TLM is fixed at a value of 0.2 F m^{-2},[52,53] in an effort to link the double layer properties of AgI and Me (hydr)oxides. It has been pointed out that the linkage can be interpreted differently,[54] leading to much higher outer capacitances of the double layer in metal (hydr)-oxides. In the CD−MUSIC approach, a value of 5 F m^{-2} for C_2 has been suggested.[23−28]

Results and Discussion

Molybdate Solution Chemistry. The formal oxidation state of molybdenum in aqueous solutions is +6 over a broad potential vs pH region. Various oxy-anions are formed whose presence and relative amount depends on the pH as well as on the total molybdate concentration.[55−57] At high-pH values (above 6), Mo is present as the tetrahedral monomeric molybdate ion MoO_4^{2-}. This can be protonated at low-pH values forming the H_2MoO_4. According to Baes and Mesmer,[55] the presence of $HMoO_4^-$ is uncertain. Decreasing the pH at concentrations above 10^{-4} M leads to the formation of the heptamolybdate polyanion, $Mo_7O_{24}^{6-}$, also known as paramolybdate, with a structure that contains MoO_6 octahedra. Depending on the acidity in solution, the heptamolybdate can be singly, doubly, or even triply protonated. At very low-pH values (below the pH range of interest), other types of Mo polymers are formed. For the conditions of this study the solution chemistry can be described by the following equilibria:

$$MoO_4^{2-} + H^+ \overset{K_1}{\longleftrightarrow} HMoO_4^- \tag{6}$$

$$MoO_4^{2-} + 2H^+ \overset{K_2}{\longleftrightarrow} H_2MoO_4 \tag{7}$$

$$7MoO_4^{2-} + 8H^+ \overset{K_3}{\longleftrightarrow} Mo_7O_{24}^{6-} + 4H_2O \tag{8}$$

$$7MoO_4^{2-} + 9H^+ \overset{K_4}{\longleftrightarrow} Mo_7O_{23}(OH)^{5-} + 4H_2O \tag{9}$$

$$7MoO_4^{2-} + 10H^+ \overset{K_5}{\longleftrightarrow} Mo_7O_{22}(OH)_2^{4-} + 4H_2O \tag{10}$$

The published values of the above-mentioned equilibrium constants have been mainly determined at very high salt levels.[55,58] However, our experiments as well as those of other groups have been done at 0.1 M ionic strength. Due to the considerable influence of the high charge of polymers on the activity coefficient, we needed new values for the equilibrium constants referring to 0.1 M ionic strength. To calculate these values, we fitted our experimental data (T = 25 °C), using equilibria 6−10 (Figure 2). We have calculated the log K_1 value for I = 0.1 M from the value in 1 M NaCl, since our data are not particularly sensitive for the log K_1 value. The other log K values were fitted. The constants K_1–K_5 are presented in Table 1, together with the values obtained from ref 55. In the calculations we used activity coefficients estimated with the Davies equation (constant = 0.2).

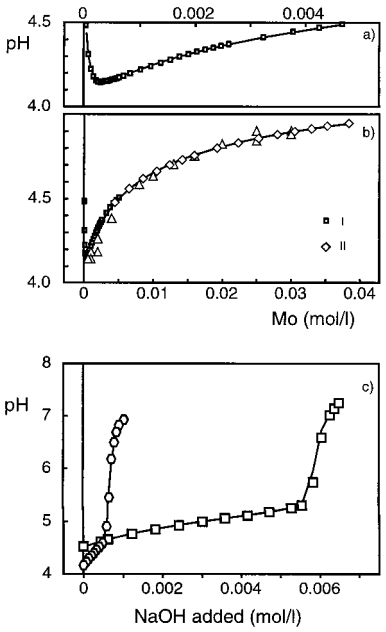

Figure 2. Variation of pH with total molybdate concentration (a,b) added as $(NH_4)_6Mo_7O_{24}$ at 25 °C and I = 0.1 M NH_4NO_3. Titration of two ammonium heptamolybdate solutions with NaOH at 25 °C in 0.1 M $NH_4^+ + Na^+$ (c). The triangles in b represent experimental data obtained from refs 34 and 59. Solid lines correspond to the calculated curve based on the equilibria of Table 1.

The speciation in the solution, based on the calculated values for the equilibrium constants, is presented in Figure 3. It is noticeable that above pH 6 only the monomeric MoO_4^{2-} ions are present in the solution at our highest Mo concentrations (≈0.01 M). At lower pH values and high total Mo concentrations ($>10^{-3}$ M), the polymers $Mo_7O_{24}^{6-}$, $Mo_7O_{23}(OH)^{5-}$, and $Mo_7O_{22}(OH)_2^{4-}$ are formed. On the basis of our formation constants of $HMoO_4$ and H_2MoO_4, we predict the dominance of MoO_4^{2-} and H_2MoO_4 as monomeric species at low concentrations $<10^{-4}$ M.

Determination of Primary Charging Parameters. Modeling of the adsorption data requires first that the charging behavior of titania is known. By modeling surface titration data, important parameters of the double layer properties can be determined, like the overall capacitance and the ion pair formation constants. Such data for our commercial titania were obtained from ref 40.

The charging mechanism of titanium oxide is described by the protonation reactions of singly, $TiOH^{-1/3}$, and doubly, $Ti_2O^{-2/3}$, coordinated groups (eqs 1 and 2). As already mentioned triply coordinated surface groups, Ti_3O^0, are inert in the normal pH range and therefore are not expected to influence the titration curves. The log K_H values of the protonation reactions 1 and 2 have been estimated recently based on the MUSIC model and the bond valence principle.[47] The difference in these values has been found to be relatively small.

TABLE 1: log K_i Values for Formation Constants of Molybdenum Species in Aqueous Solutions at 25 °C (Equations 6−10)

medium	$HMoO_4$	H_2MoO_4	$Mo_7O_{24}^{6-}$	$HMo_7O_{24}^{5-}$	$H_2Mo_7O_{24}^{4-}$	source
0.1 M NH_4NO_3	3.60	7.82	52.65	58.11	62.24	this study
1 M NaCl	3.55	7.20	52.81	57.39	61.02	ref 55
3 M $NaClO_4$	3.89	7.50	57.74	62.14	65.68	ref 55
intrinsic values	4.16[a]	8.49	52.65	59.46	64.71	this study

[a] Calculated from the data in 1 M NaCl.

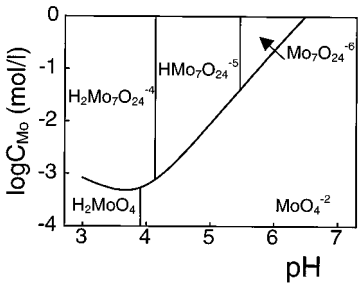

Figure 3. Predominant molybdenum species at 25 °C and I=0.1 M. The lines represent conditions where the predominant species in adjacent regions contain equal amounts of $Mo^{(vi)}$.

Because of the uncertainty, we simplified protonation by assuming equal values for the log K_H of reactions 1 and 2. In that case the log K_H values are equal to the PZC value of the (hydr)oxide,[23,47] if symmetrical ion pair formation is assumed.

The formation of ion pairs can be described by the following reactions:

$$TiOH^{-1/3} + NH_4^+ \xleftrightarrow{K_{NH4+}} TiOH^{-1/3} - NH_4^+ \quad (11)$$

$$TiOH_2^{+2/3} + NO_3^- \xleftrightarrow{K_{NO3-}} TiOH_2^{+2/3} - NO_3^- \quad (12)$$

$$Ti_2O^{-2/3} + NH_4^+ \xleftrightarrow{K_{NH4+}} Ti_2O^{-2/3} - NH_4^+ \quad (13)$$

$$Ti_2OH^{+1/3} + NO_3^- \xleftrightarrow{K_{NO3-}} Ti_2OH^{+1/3} - NO_3^- \quad (14)$$

In the present study, we use asymmetrical ion pair formation due to a small difference between PZC (6.2) and IEP (6.6). This leads to the adoption of a value of 6.6 for the protonation constants log K_{H1} and log K_{H2}, slightly higher than the PZC.

For the calculation of the surface charge, a value for the site density (N_s) is also required. Calculated N_s values for the different crystal faces of both anatase and rutile can be found in ref 46. The 010 and 011 are often assumed to be the predominant faces of anatase.[60] However, also the 001 face can be found.[61] Since the picture is not so clear and the variation in site densities for different crystal faces is not large (between 5.2 and 7.0 nm^{-2} for each type of surface groups), we used an intermediate value of 6 singly and 6 doubly coordinated sites/nm^2 as a first approach. We note that the charging behavior of titania is not very sensitive to the precise value of the total site density. The adsorption capacity of molybdate ions is, however, sensitive to this value. For this reason N_S was determined later more accurately in the modeling of Mo adsorption.

A good description of the titration data was obtained (Figure 4) by using a value of 0.9 F m^{-2} for the overall Stern capacitance and asymmetric ion pair formation, with $K_{NH4+} = -0.4$ and $K_{NO3-} = -1.3$. The basic Stern model was used for the calculations. It must be mentioned here that for the description of the experiments where sodium nitrate was used as the background electrolyte, a value of $K_{Na^+} = -0.5$ is used for Na^+. This is a mean value calculated after fitting a large number of titration data of titanium oxide found in the literature.[62]

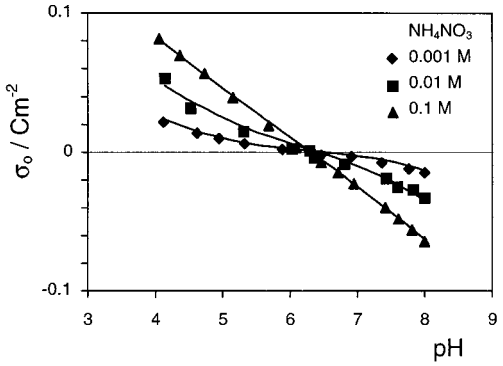

Figure 4. Charging behavior of titania (Degussa P25) at three electrolyte concentrations. Data points correspond to experimental data, and lines correspond to the calculated curves, using the basic Stern model. Parameter values are given in the text.

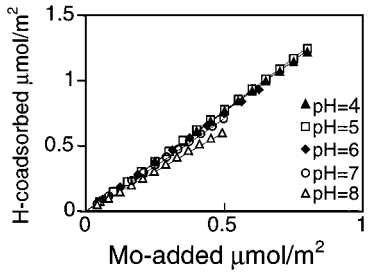

Figure 5. Proton coadsorption as a function of molybdate adsorption at pH 4.0, 6.0, and 8.0. Points represent experimental data, and solid lines correspond to calculated curves by applying the CD−MUSIC approach, assuming a combination of bidentate and monodentate complexes. $T = 25$ °C; $I = 0.1$ M $NaNO_3$.

Low Molybdate Adsorption Levels. The choice of separating the adsorption study of molybdenum into low and high adsorption levels was based on the polymerization of molybdates at high concentrations. The study at low Mo loading is necessary for the calculation of the contribution of Mo monomer adsorption at high Mo loading.

Determination of Adsorption Parameters. The charging behavior of titania, as determined in the previous paragraph, is expected to influence strongly its adsorption capacity for the molybdates. A high positive surface charge at low-pH values enhances the adsorption capacity for anions, like MoO_4^{2-}. Therefore, the pH can be considered as the most important parameter influencing the adsorption isotherm. As mentioned in the Introduction, correct description of the pH dependency of adsorption can adequately be performed with modeling proton−ion adsorption stoichiometry data.[36] Recently, it has been shown[38] that in the case of only one type of adsorbed species, the proton−ion stoichiometry is independent of the affinity constant once the charging parameters have been found (titration data). The proton−ion stoichiometry is then only related to the location of the charge of the species in the electrostatic potential profile. In case of inner sphere complex formation, the location is determined by the charge distribution in the complex.

We performed proton ion titrations, for studying the molyb-

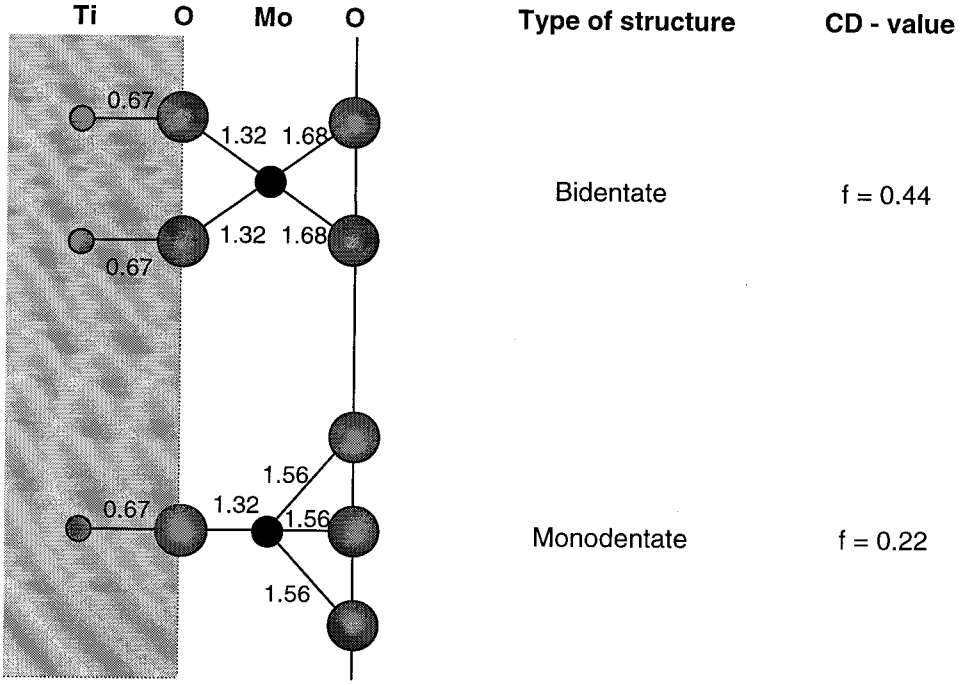

Figure 6. Schematic representation of the suggested structure of the adsorbed molybdate complexes based on calculations with the CD−MUSIC approach. An asymmetrical charge distribution of the molybdate atom over the surrounding oxygens has been found. The numbers indicate the bond valences that oxygens receive from the coordinated cations.

date adsorption pH dependency, at various pH values (4.0, 5.0, 6.0, 7.0, and 8.0). The experimental results determined at pH 4.0, 6.0, and 8.0, are presented in Figure 5 with points. It is noticed that the coadsorption of protons is not stoichiometric. If the surface behavior was Nernstian, a stoichiometry of 2 would be expected for a bivalent ion like MoO_4^{2-}, if all charge is attributed to the surface (point charge). However, the actual value is approximately 1.5, showing a less strong interaction of MoO_4^{2-} ions with the protonated surface.

We applied the CD−MUSIC approach with the three plane model option to calculate the proton coadsorption for the data in the pH range 4.0−8.0. The value of the outer capacitance C_2 was fixed at 5 F m^{-2}, based on previously reported results from related studies.[23−28] The value for C_1 (1.1 F m^{-2}) was calculated using eq 5, based on the overall capacitance C of 0.9 F m^{-2}, found from the modeling of the titration curves. First, we analyzed the proton ion titration data, assuming one type of surface complex. A relatively high CD value of approximately f 0.46 is found. This points to the formation of bidentate complexes.[38] The CD value changes however with pH, which is an indication of the presence of more than one type of surface species. The data showed a lower CD value at high pH. This lower value can be understood assuming a contribution of monodentate complexes, since these complexes attribute less charge to the surface. In the case of the presence of only one type of surface species, the proton−ion adsorption stoichiometry only depends of the charge distribution in that particular species. However, if two surface species are present, the stoichiometry will also depend on the relative presence of both species. It implies that both corresponding binding constants are needed to be fitted too. At pH = 8, 5% of the added Mo was found in solution at the end of the experiment. This was taken into account when fitting the data. Using this approach, the fitting achieved was quite good for all the pH values studied. The adsorption reactions are defined as

$$\mathrm{TiOH}^{-1/3} + \mathrm{H}^{+} + \mathrm{MoO_4}^{2-} \overset{K_{M1}}{\longleftrightarrow} \mathrm{TiOMoO_3}^{-4/3} + \mathrm{H_2O} \quad (15)$$

$$2\mathrm{TiOH}^{-1/3} + 2\mathrm{H}^{+} + \mathrm{MoO_4}^{2-} \overset{K_{M2}}{\longleftrightarrow} \mathrm{Ti_2O_2MoO_2}^{-2/3} + 2\mathrm{H_2O} \quad (16)$$

The number of common ligands in a monodentate complex are half of the number in a bidentate complex. Therefore it is assumed that the charge attribution of the monodentate complex will be half that of the bidentate complexes. The result of the fitting yields a charge attribution of $f = 0.44 \pm 0.01$ for the bidentate surface complex. The value is $f = 0.22$ for the monodentate complex. In case of symmetrical distribution of the charge of the Mo(VI) ion in both types of surface complexes (bi- and monodentate), values of respectively 0.5 and 0.25 are expected. The actual values are slightly lower; i.e., slightly less Mo charge is attributed to the common oxygens of the surface complex and slightly more Mo charge to the outer oxygens. The reason for this can be traced by expressing the CD value f in the bond valence of the Mo−O bonds. For the Mo−O bond directed to the surface a value of about 1.32 is found (see Figure 6). The combination of this value with the bond valence of the Ti−O bond (0.67) shows that the common oxygen(s) is (are) fully neutralized. This is considered as the most stable configuration.[51] Charge oversaturation of the common oxygens is not allowed,[51] which would have occurred if Mo had distributed the charge symmetrically over its ligands. The above analysis illustrates that geometry may strongly affect the CD value in the surface complex. Since the CD value in the MUSIC approach largely determines the coadsorption of protons and corresponding pH dependency of adsorption, it also shows that a tight relationship exists between the geometry and the macroscopic adsorption behavior.

Having determined the charge distribution as well as a first estimate of the intrinsic log K_M values of the adsorbed species, we applied our evaluation by describing the pH dependency of the molybdate adsorption over a large pH range, at three different Mo concentrations. The previous analysis of the proton−ion titrations (Figure 5) was almost insensitive to the value of the site density, N_S, in the physically realistic range of

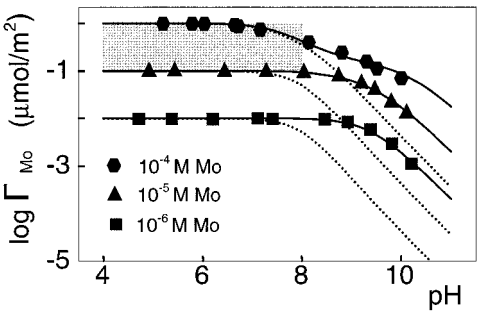

Figure 7. Adsorption of molybdenum on titania (2.5 g/L) as a function of pH, at three different initial concentrations ($10^{-6} - 10^{-4}$ M). Data points represent experimental data, and dashed (solid) lines correspond to calculated curves without (with) considering the presence of high-affinity sites. $T = 25$ °C; $I = 0.1$ M $NaNO_3$.

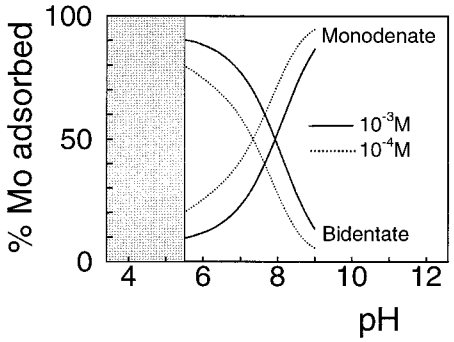

Figure 8. Calculated relative surface speciation of molybdenum on titania in 0.1 M $NaNO_3$, as a function of pH at two different initial concentrations. The gray block indicates the area of increasing polymerization.

$5-7$ sites nm^{-2}. The adsorption data of Figure 7 are more sensitive, and we used this phenomenon to optimize the site density parameter, yielding $N_S = 5.6 \pm 0.2$ sites nm^{-2}. This value is quite close to the calculated values of 5.6 nm^{-2} for the 010 and 5.2 nm^{-2} for the 011 face of anatase,[47] suggesting that these faces may be predominant in the material used.

The gray area in Figure 7 indicates approximately the experimental window used in the proton−ion titration experiment of Figure 6 (pH = 4.0−8.0 and $\Gamma \approx 0.1-1$ μmol m^{-2}). The predicted adsorption is adequate for these conditions. At the low Mo levels (10^{-6} and 10^{-5} M) and at the high Mo level above pH 8.0 the experimental adsorption is higher than the predicted one. This result shows that probably a high affinity adsorption takes place in low adsorption levels. This phenomenon has been noticed in other systems (e.g., 25). High affinity at high-pH values could be due to presence of cationic impurities that act cooperatively[63,64] or due to presence of high-affinity sites.[24]

Looking for impurities, we analyzed, with ICP-MS, supernatants of the adsorption experiments, over the whole pH range, for a whole series of elements. The analysis showed no considerable amounts of impurities (<50 μg L^{-1}). Since the first possibility of a potential cooperative adsorption seemed unrealistic, we adopted the idea of the presence of high-affinity sites on the titania surface. Using the same adsorption reactions as 15 and 16 and the charge distribution obtained for the adsorbed species, we derived the site density of the high-affinity sites and the corresponding affinity constants, assuming that the high-affinity sites had the same $\Delta \log K_M$ as the low-affinity sites. The previously determined parameters as well as the quality of the fitting of the proton coadsorption data did not change considerably. The calculated values for the affinity constants and the site density are compiled in Table 2. The lines in Figures 6 and 7 are calculated using this parameter set. A very low value for the site density of the high-affinity sites ($Ti_hOH^{-1/3}$) was found (0.1 ± 0.02 nm^{-2}). Such a very low value cannot be easily related to a known ideal surface structure of titania. It is more likely that these sites are related to, e.g., defects. Finally, it must be mentioned that taking into account only one type of adsorbed complex at the high-affinity sites led to less description of the data. For this reason we adopted also for these sites two kinds of surface complexes (monodentate and bidentate).

Surface Speciation. The surface speciation of the adsorbed complexes is strongly pH dependent (Figure 8). At low-pH values, the dominant species is the bidentate one, whereas at high-pH values the monodentate structure is favorable. This can be understood if we consider the influence of the electrostatic field to each structure. In the bidentate species, more negative charge is located at the surface than in the monodentate species. This is due to the higher number of common oxygen ligands in the bidentate (2) vs the monodentate (1) species. At low-pH values, where the surface is positively charged, the species that attributes most of its negative charge to the surface is preferable and this is the bidentate complex. At high-pH values where the surface is negatively charged, the species which keeps most of its negative charge away from the surface is preferred, i.e., the monodentate complex.

As also shown in Figure 8, the increase of the Mo loading favors the binding of the bidentate complex against the monodentate one since the negative charge in the 1-plane becomes an increasing limiting factor. The species with the lowest input of charge in this region (1-plane) is preferred, i.e., the bidentate complex (see also ref 26).

High Molybdate Adsorption Levels. Once the adsorption parameters for low molybdate concentrations have been determined, our approach can be extended to the study of the adsorption of molybdates on titania in high Mo concentrations. As Figure 3 shows, at concentrations higher than 10^{-4} to 10^{-3} M and low-pH values polymeric species are formed in the solution. If polymers are adsorbed, these species are in competition with the Mo monomers, for instance due to electrostatic interaction. This means that describing the adsorption at high concentrations demands that, apart from the molybdenum polymers, also the monomers should be taken into account.

Some experimental data for Mo adsorption at high concentra-

TABLE 2: Surface Parameters (TP Model) Used in the Description of the Adsorption Data[a]

	value			value	
parameter	low-affinity sites	high-affinity sites	parameter	low-affinity sites	high-affinity sites
C_1 (F m^{-2})	1.1	1.1	N_S (nm^{-2})	5.6	0.1
C_2 (F m^{-2})	5.0	5.0	log K_{M1}	11.9	15.2
log K_H	6.6	6.6	log K_{M2}	19.2	22.5
Log K_C	−0.5,[b] −0.4c	−0.5[b]	log K_{M3}	173	
log K_A	−1.3	−1.3			

[a] CD values of the adsorbed complexes are given in Figure 6. [b] Na^+. [c] NH_4^+.

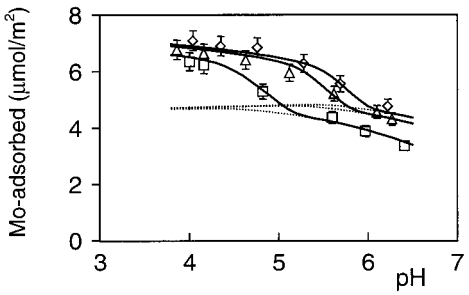

Figure 9. Adsorption of molybdenum on titania (2, 15, 25 g/L) as a function of pH, at three different initial concentrations (0.001, 0.01, and 0.02 M). Points represent experimental data, and solid lines correspond to calculated curves. The dashed lines are calculated by omitting the presence of adsorbed molybdate polymers. $T = 25$ °C; $I = 0.1$ M NH_4NO_3.

tions were available in the literature.[34] However, most of the data are not in the pH range where polymerization is significant. Analysis showed that the data are possibly not accurate enough since a low solid-solution ratio was used. We therefore designed own experiments, covering especially the low-pH range. We performed adsorption edges at three initial molybdenum concentrations (10^{-3}, 10^{-2}, and 2×10^{-2} M), at a range of pH 4.0−6.5. The experimental results are presented in Figure 9 (points). Under these conditions, as can be seen in Figure 3, both monomers and polymers are present in the solution. Polymers are mainly found in the form of $Mo_7O_{23}(OH)^{5-}$ as well as the doubly protonated $Mo_7O_{22}(OH)_2^{4-}$. The dashed lines in Figure 9 represent model calculations done by extrapolating the monomeric adsorption behavior to high Mo concentrations, ignoring the adsorption of polymeric molybdenum species. At values above about pH 6 the adsorption is described well contrary to the lower pH range. This indicates that molybdenum polymers must be necessarily included in the analysis.

Determination of Adsorption Parameters. As already mentioned, a very important aspect of the CD−MUSIC approach is the charge distribution. Ions are assumed to have a spatial distribution of their charge in the electrostatic potential profile of the interface. This aspect may also be useful in our case where large ions, like the polymers, must be handled. The structure of the polymer is also expected to be important due to size and steric constraints.

Some useful information about the structure of the $Mo_7O_{24}^{6-}$ polyanion can be obtained from the literature.[56,57] It is believed that it is a ring structure consisting of seven MoO_6 octahedra, as shown in Figure 10. This structure was derived from analysis of the crystal structure of potassium heptamolybdate tetrahydrate and ammonium heptamolybdate tetrahydrate.[65,66] The lengths of the Mo−Mo and Mo−O bonds are given in the literature.[65,66] On the basis of those results, we can have a rough estimation about the size of the $Mo_7O_{24}^{6-}$ polyanion. It can cover, as a maximum, an area of about 0.8 ± 0.1 nm^2. This means that if the ring structure is adsorbed in the interface parallel to the surface, each polymer will cover approximately 14 (6 or 8 singly and 8 or 6 doubly coordinated) reactive surface sites. A schematic representation is shown in Figure 11.

On the basis of the knowledge of the structure and with the inclusion of the known adsorption of the Mo monomers, we modeled our data, applying the CD−MUSIC approach to the adsorption of polymers. The best fit was obtained by assuming outer sphere formation for the polyanion, interacting with a high number (12−14) of protonated surface groups. The high number of sites needed in the modeling supports the assumption of an

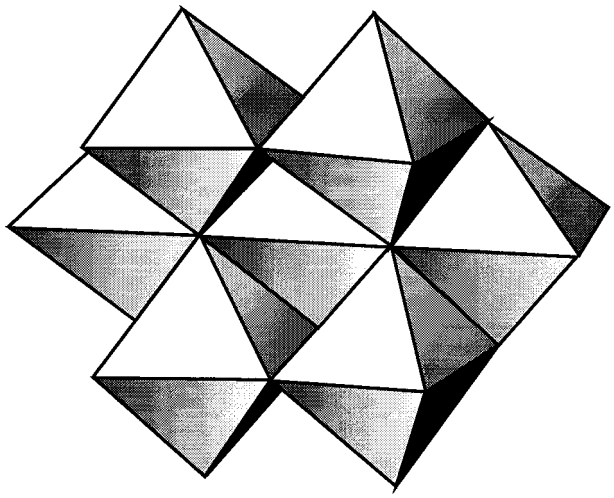

Figure 10. Structure of the heptamolybdate $Mo_7O_{24}^{6-}$ ion.[57]

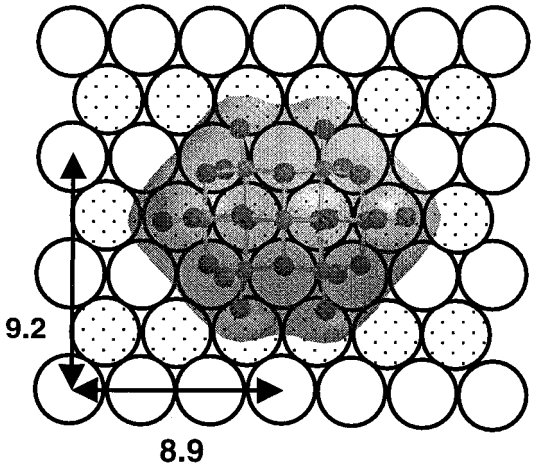

Figure 11. Projection of an adsorbed molybdate polymer on the titania surface, having rows of singly and doubly (dotted) coordinated surface groups. The polymer geometry was calculated using the Mo−Mo distances of potassium molybdate and Mo−O distances based on the bond valence distance approach.

outer sphere with a position of the ring structure parallel to the surface (Figure 11).

The charge of the adsorbed polymer is assumed to be distributed in the interface over the outer two planes. As can be seen in Figure 9, the calculated adsorption edges (solid lines) are in good accordance with the experimental data. It must be noticed that the use of only one type of adsorbed species is enough for the good description. The data are not particularly sensitive for the choice of the number of protons bound to the Mo polyanion. We choose the protonated $HMo_7O_{24}^{5-}$ as outer sphere complex, since it is the most dominant species in the pH and Mo concentration range (see Figure 3). A further protonation to $H_2Mo_7O_{24}^{4-}$ may in principle occur as a result of the high negative potential developed in the inner plane by the accumulation of the negatively charged molybdate species, attracting protons strongly. This has not been accounted for. The adsorbed $HMo_7O_{24}^{5-}$ can be seen as a combination of adsorption of $Mo_7O_{24}^{6-}$ and one H^+. The charge of the $Mo_7O_{24}^{6-}$ part of the polymer is assumed to be distributed symmetrically (−3, −3) between the 1- and 2-plane. The proton is located at the plane with the most negative potential, i.e., in the 1-plane. Modeling shows that under these conditions a portion of the positive charge of the surface groups is transferred from the surface (0-plane) to the 1-plane. This may point to the

formation of strong hydrogen bonds between the surface hydroxyls and the oxygens of the polymer, where the last act as proton acceptors. Particularly, it was found that the +14 charge of the surface protons of the covered groups is distributed (+12.3, +1.7 vu) between the surface and the 1-plane. This means that about 0.1 vu per H bond is attributed to the 1-plane. Charge transfer due to H bonds has also been suggested for the adsorption of some organic acids on goethite, where hydrogen bonds form between the surface of the hydroxide and the adsorbed organic molecules.[28]

The formulation of the adsorption reaction is the following:

$$6\mathrm{TiOH}^{-1/3} + 8\mathrm{Ti_2O}^{-2/3} + 23\mathrm{H}^{+} + 7\mathrm{MoO_4}^{2-} \xleftrightarrow{K_{M3}} (6\mathrm{TiOH_2}^{+2/3})(8\mathrm{Ti_2OH}^{+1/3}) - \mathrm{Mo_7O_{23}(OH)}^{5-} + 4\mathrm{H_2O} \quad (17)$$

The value of log K_{M3} is given in Table 2. The combination of 6 singly and 8 doubly coordinated surface groups instead of 8 and 6, respectively, resulted in a slightly better description. With the 6/8 combination more singly coordinated sites remain for Mo inner sphere complex formation.

In contrast to inner sphere adsorption, which involves only singly coordinated groups, outer sphere complexes can form pairs with positively charged singly and doubly coordinated groups. A good fit was only possible if a sufficiently large part of the negative charge of the polymer was attributed to the 2-plane, pointing to an outer sphere complex formation. At the lower adsorption level (10^{-3} M), polymers have almost no influence in the adsorption, in the pH range 5.5−6.5. This gave the opportunity of an additional estimation of the N_S value since in this range it was the only adjustable parameter. The value that described those data best equals 5.6 sites nm^{-2}, confirming our previous calculation done in the low adsorption levels.

It must be mentioned that the combination of the parameters achieved for the description of polymer adsorption may not be a unique one. However, some important characteristics, like the location of the polyanion and the type of complex it forms, are not flexible.

Finally, it should be noticed that in view of the recent finding[21] of the formation and adsorption of an alumino-heteropolymolybdate species on the alumina surface, we checked our system looking for a possible similar situation. However, the measured (with ICP-MS) dissolution of the titanium oxide was negligible even at low-pH and high-Mo-concentration values, showing that the formation of such a species is insignificant.

Polymer−Monomer Competition. In Figure 12, the speciation of a titania system in equilibrium with a 10^{-2} M molybdenum solution is presented. Figure 12a refers to the solution and Figure 12b to the adsorbed species. Above pH 6, exclusively adsorption of monomers occurs (Figure 12b). The interaction with the singly coordinated titania surface sites reaches its physical maximum around pH 6.5. As shown in Figure 12a, the concentration of the monomers in solution decreases considerably below pH 5.5, whereas the polymer concentration increases. It points to a strong competition between these two forms. As a result, most of the adsorbed molybdenum is present in the polymeric form. However, it must be noticed that although the concentration of the monomers significantly decreases at low-pH values, the decrease of the adsorbed molybdenum found in monomers is much smoother and does not become negligible even at pH values where almost no monomers are found in the solution. This observation suggests a favorable adsorption of the MoO_4^{2-} ions compared to the $Mo_7O_{23}(OH)^{5-}$ polyanions.

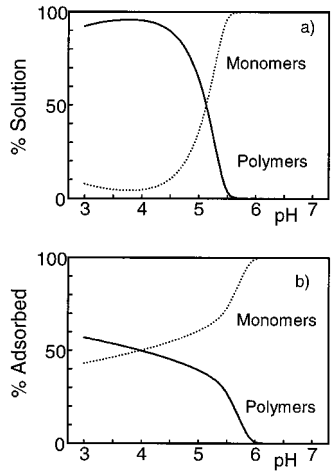

Figure 12. (a) Calculated relative distribution of molybdenum in monomers and polymers in 10^{-2} M equilibrium solution. $I = 0.1$ M NH_4NO_3. (b) Calculated relative distribution of adsorbed molybdenum in monomers and polymers at the 10^{-2} M Mo level in solution. $I = 0.1$ M NH_4NO_3.

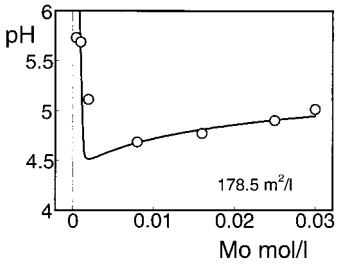

Figure 13. Variation of pH, measured after adsorption, with total molybdate concentration added as $(NH_4)_6Mo_7O_{24}\cdot 4H_2O$ to a titania suspension of 178.5 m^2 L^{-1}, at 25 °C and $I = 0.1$ M NH_4NO_3. Data points represent experimental data obtained from ref 34, and the solid line corresponds to the calculated curve.

The above-presented calculated speciation is in accordance with related spectroscopic studies. Raman and Fourier infrared spectroscopy have been used for determining the structure of the adsorbed molybdates in titania supported catalysts, in both dried and calcined state.[31] The results indicate that the nature of the surface species depends on the loading and the pH of the impregnation suspension. It has been found that at low coverage as well as in catalysts prepared at high-pH values, the tetrahedral monomer is the main surface species. In catalysts prepared at low-pH values having high Mo loading, octahedral polymeric species are formed at the expense of the tetrahedral molybdates, in accordance with the model predictions. Characteristically, a sharp change in the catalyst's Raman peak frequencies is observed at pH 5.5 due to the formation of the octahedral polymeric species. This is in full agreement with our modeling which predicts around this pH value the start of the formation of Mo polymers on the titania surface (see Figure 12). For a detailed interpretation of the structure of the adsorbed complexes, information provided by advanced techniques such as XAFS[17−20] or NMR[20−22] is necessary. At present, no such information for the studied system is available.

Model Predictions. Having determined the adsorption parameters over a wide range of molybdate concentrations, the modeling can be further tested by comparing predictions of the model with relevant experimental data.

In Figure 13, the variation in pH, measured after adsorption of different initial molybdate concentrations, is presented. The predicted line according to the model is in good agreement with the experimental data. The final pH of the system after

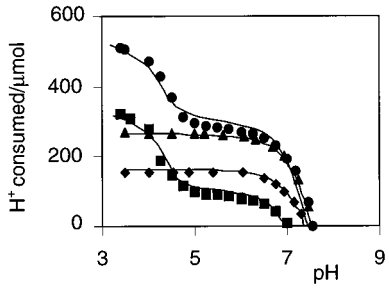

Figure 14. Hydrogen ions consumed by the protonation of surface groups as well as by the equilibrium reactions taking place in the solution. (◆) solution NH_4NO_3, (▲) suspension NH_4NO_3/TiO_2, (■) solution $Mo_xO_y(OH)_w^{z-}$ ions/NH_4NO_3, (●) suspension $Mo_xO_y(OH)_w^{z-}$ ions/NH_4NO_3/TiO_2. $T = 25$ °C; $I = 0.1$ M. Data points represent experimental data obtained from ref 34. Solid lines correspond to model calculated curves, using the parameter values presented in Tables 1 and 2.

adsorption is a complicated function of different parameters, like the initial pH before the adsorption (see Figure 3), depolymerization of the added ammonium heptamolybdate, and the coadsorption of protons. In Figure 14 titrations of different solutions and suspensions are presented. Details are given in the figure legend. For a good description of these data, a correct molybdenum solution chemistry, titania charging behavior and pH dependent adsorption are required. The quite good agreement between the predicted lines and the experimental data corroborates the validity of the modeling.

Conclusions

The following conclusions can be drawn from the present study:

(i) The adsorption of molybdate monomers and polymers on titania surface can be described very well by the CD−MUSIC model, over a large pH and Mo(VI) concentration range.

(ii) The titania surface is not considered homogeneous but characterized by the presence of different types of surface groups, namely, singly ($TiOH^{-1/3}$), doubly ($Ti_2O^{-2/3}$), and triply (Ti_3O^0) coordinated.

(iii) Surface complexes are not treated as point charges. The interfacial charge allocation is determined by their structure. In the entire parameter range, Mo monomers (MoO_4^{2-}) are adsorbed, reacting with the singly coordinated surface groups, forming inner sphere complexes. The surface speciation is pH dependent. At high pH a monodentate structure is favored versus a bidentate one, which becomes predominant at low-pH values.

(iv) At high Mo concentrations and below pH 5.5 the polyanion $Mo_7O_{23}(OH)^{5-}$ is additionally adsorbed as an outer sphere surface complex, covering approximately 12−14 reactive surface groups.

(v) At very low Mo levels, high-affinity adsorption of molybdates on titania surface is observed.

Appendix

In Table 3 the table of species is presented for a Mo−titania system (low-affinity sites only). Formation of each surface species is defined in terms of components (columns), being components in solution, surface components (surface groups), and electrostatic components ($\exp(-F\Psi_i/RT)$), with $i = 0$, 1, and 2, standing for the corresponding planes). The concentration [S] (mol L^{-1}) of a surface species can be calculated by reading the table horizontally and using the following general expression:

$$[S] = 10^{\log K} \prod_k [C_k]^{n_k} \qquad \text{(A)}$$

where C_k is the component's concentration (mol L^{-1}) and n_k the coefficient given in the table. The expression of log K is given in the last column of Table 3 as a function of various log K values whose meaning and value can be found in the text (see Table 2). All log K values are based on intrinsic constants,

TABLE 3: Surface Speciation for the Adsorption of Molybdates on Titania Surface[a]

	dissolved component				surface component		electrostatic component			
surface species	H^+	Na^+ (NH_4^+)	NO_3^-	MoO_4^{2-}	$TiOH^{-1/3}$	$Ti_2O^{-2/3}$	$e^{-F\Psi 0/RT}$	$e^{-F\Psi 1/RT}$	$e^{-F\Psi 2/RT}$	log K
$TiOH^{-1/3}$	0	0	0	0	1	0	0	0	0	0
$Ti_2O^{-2/3}$	0	0	0	0	0	1	0	0	0	0
$TiOH_2^{+2/3}$	1	0	0	0	1	0	1	0	0	log K_H
$Ti_2OH^{+1/3}$	1	0	0	0	0	1	1	0	0	log K_H
$TiOH^{-1/3} - NH_4^+$ (Na^+)	0	1	0	0	1	0	0	0	1	log $K_{Na^+(NH_4^+)}$
$Ti_2O^{-2/3} - NH_4^+$ (Na^+)	0	1	0	0	0	1	0	0	1	log $K_{Na\ (NH_4^+)}$
$TiOH_2^{+2/3} - NO_3^-$	1	0	1	0	1	0	1	0	1	log $K_{NO_3^-}$ + log K_H
$Ti_2OH^{+1/3} - NO_3^-$	1	0	1	0	0	1	1	0	1	log $K_{NO_3^-}$ + log K_H
$TiOMo\ O_3^{-4/3}$	1	0	0	1	1	0	0.34	1.34	0	log K_{M1}
$Ti_2O_2MoO_2^{-2/3}$	2	0	0	1	2	0	0.68	0.68	0	log K_{M2}
$(TiOH_2^{+2/3})_6(Ti_2OH^{+1/3})_8Mo_7O_{23}(OH)^{5-}$	23	0	0	7	6	8	12.3	0.3	3	log K_{M3}
sum	Σ_1	Σ_2	Σ_3	Σ_4	Σ_5	Σ_6	Σ_7	Σ_8	Σ_9	

[a] Surface speciation at high-affinity sites is omitted in this example table. It is described by the same equations, with the exception of the absence of the last polymeric species.

$$\Sigma_1 = H^+(t) - OH^-(t) \qquad \text{(A-1)}$$

$$\Sigma_2 = Na^+(t) \text{ or } NH_4^+(t) \qquad \text{(A-2)}$$

$$\Sigma_3 = NO_3^-(t) \qquad \text{(A-3)}$$

$$\Sigma_4 = MoO_4^{2-}(t) \qquad \text{(A-4)}$$

$$\Sigma_5 = \rho A N_{S,1} \qquad \text{(A-5)}$$

$$\Sigma_6 = \rho A N_{S,2} \qquad \text{(A-6)}$$

$$\Sigma_7 = \rho A/F(\sigma_0 - \Sigma z_j F N_{S,j}) \qquad \text{(A-7)}$$

$$\Sigma_8 = \rho A/F\sigma_1 \qquad \text{(A-8)}$$

$$\Sigma_9 = \rho A/F\sigma_2 \qquad \text{(A-9)}$$

$$\sigma_0 = C_1(\Psi_0 - \Psi_1) \qquad \text{(A-7a)}$$

$$\sigma_1 = C_2(\Psi_1 - \Psi_2) - C_1(\Psi_0 - \Psi_1) \qquad \text{(A-8a)}$$

$$\sigma_2 = C_2(\Psi_2 - \Psi_1) \pm \frac{1}{2}\sqrt{8000\epsilon_0 e_r RT}\sqrt{\sum_i C_i(e^{-z_i F\Psi_2/RT} - 1)} \qquad \text{(A-9a)}$$

adjusted for activity corrections in the case of $I \neq 0$. The activity coefficients were estimated with the Davies equation (constant $= 0.2$). The calculation of the coefficients for the electrostatic components has also been described in the text (see CD−MUSIC approach).

The parameters in the summation terms in Table 3 are as follows: ρ, the solid solution ratio (kg L^{-1}); A, the specific surface area (m^2 kg^{-1}); F, the Faraday constant (C mol^{-1}); σ_0, σ_1, and σ_2, the charges (C m^{-2}) in respectively the 0-, 1-, and 2-planes; z_j the charge of the surface reference groups $TiOH^{-1/3}$ and $Ti_2O^{-2/3}$; $N_{S,j}$, the site densities (mol m^{-2}) of the corresponding surface groups; Ψ_0, Ψ_1, and Ψ_2, the electrostatic potential (V) of respectively the 0-, 1-, and 2-planes; C_1, the capacitance (C V^{-1} m^{-2}) of the layer between the 0- and 1-plane; C_2, the capacitance (C V−^{1} m^{-2}) of the layer between the 1- and 2-plane; ϵ_0, the absolute dielectric constant (C V^{-1} m^{-2}); ϵ_r, the relative dielectric constant; R, the gas constant (J mol^{-1} K^{-1}); T, the absolute temperature (K); C_i, the concentrations of the dissolved electrolyte solution species with valence z_i. Values of the above-mentioned parameters can be found in the text (Table 2).

References and Notes

(1) Lycourghiotis, A. In *Preparation of Catalysts VI*; Poncelet, G., Martens, J., Delmon, B., Jacobs, P. A., Grange, P., Eds.; Elsevier: Amsterdam, 1995; p 95.

(2) Schwarz, J. A.; Contescu, C.; Contescu, A. *Chem. Rev.* **1995**, *95*, 477.

(3) Hingston, F. J. In *Adsorption of inorganics at Solid−Liquid interfaces*; Anderson, M. A., Rubin, A. J., Eds.; Ann Arbor Science: Ann Arbor, MI, 1981; Chapter 2.

(4) James, R. O.; Parks, G. A. In *Surfaces and Colloid Science*; Matijevic, E., Ed.; Plenum: New York, 1982; Vol. 12, Chapter 2.

(5) Sposito, G. *The Surface Chemistry of Soils*; Oxford University Press: New York, 1984.

(6) Barrow, N. J. In *Reactions with Variable Charge Soils*; Nijhoff: Dordrecht, The Netherlands, 1987.

(7) Dzombak, D. A.; Morel, F. M. M. In *Surface Complexation Modeling: Hydrous Ferric Oxide*; Wiley: New York, 1990.

(8) Davis, J. A.; Kent, D. B. In *Mineral−Water Interface Geochemistry: Reviews in Mineralogy*; Hochella, M. F., White, A. F., Eds.; Mineralogical Society of America: Washington, DC, 1990; Vol. 23, p 177.

(9) Goldberg, S. In *Advances in Agronomy*; Sparks, J. L., Ed.; Academic Press: New York, 1992; Vol. 47, p 233.

(10) Stumm, W. *Chemistry of the Solid-water Interface*; Wiley: New York, 1992.

(11) Bourikas, K.; Matralis, H. K.; Kordulis, Ch.; Lycourghiotis, A. *J. Phys. Chem.* **1996**, *100*, 11711.

(12) Charmas, R. *Langmuir* **1999**, *15*, 5635.

(13) Venema, P.; Hiemstra, T.; Van Riemsdijk, W. H. *J. Colloid Interface Sci.* **1996**, *181*, 45.

(14) Tejedor-Tejedor, M. I.; Anderson, M. A. *Langmuir* **1990**, *6*, 602.

(15) Biber, M. V.; Stumm, W. *Environ. Sci. Technol.* **1994**, *28*, 763.

(16) Fendorf, S.; Eick, M. J.; Grossl, P.; Sparks, D. L. *Environ. Sci. Technol.* **1997**, *31*, 315.

(17) Spadini, L.; Manceau, A.; Schindler, P. W.; Charlet, L. *J. Colloid Interface Sci.* **1994**, *168*, 73.

(18) Bargar, J. R.; Brown, G. E., Jr.; Parks, G. A. *Geochim. Cosmochim. Acta* **1997**, *61*, 2617.

(19) Towle, S. N.; Brown, G. E. Jr.; Parks, G. A. *J. Colloid Interface Sci.* **1999**, *217*, 299.

(20) Shelimov, B.; Lambert, J.-F.; Che, M.; Didillon, B. *J. Catal.* **1999**, *185*, 462.

(21) Carrier, X.; Lambert, J.-F.; Che, M. *J. Am. Chem. Soc.* **1997**, *119*, 10137.

(22) Carrier, X.; d'Espinose de la Caillerie, J.-B.; Lambert, J.-F.; Che, M. *J. Am. Chem. Soc.* **1999**, *121*, 3377.

(23) Hiemstra, T.; Van Riemsdijk, W. H. *J. Colloid Interface Sci.* **1996**, *179*, 488.

(24) Venema, P.; Hiemstra, T.; Van Riemsdijk, W. H. *J. Colloid Interface Sci.* **1996**, *183*, 515.

(25) Venema, P.; Hiemstra, T.; Van Riemsdijk, W. H. *J. Colloid Interface Sci.* **1996**, *192*, 94.

(26) Hiemstra, T.; Van Riemsdijk, W. H. *J. Colloid Interface Sci.* **1999**, *210*, 182.

(27) Rietra, P. J. J.; Hiemstra, T.; Van Riemsdijk, W. H. *J. Colloid Interface Sci.* **1999**, *218*, 511.

(28) Filius, J. D.; Hiemstra, T.; Van Riemsdijk, W. H. *J. Colloid Interface Sci.* **1997**, *195*, 368.

(29) Segawa, K.; Kim, D. S.; Kurusu, Y.; Wachs, I. E. In *Proceedings, 9th International Congress on Catalysis*; Phillips, M. J., Ternan, M., Eds.; Chemical Institute of Canada: Ottawa, 1988; p 1960.

(30) Kim, D. S.; Kurusu, Y.; Wachs, I. E.; Hardaste, F. D.; Segawa, K. *J. Catal.* **1989**, *120*, 325.

(31) Ng, K. Y. S.; Gulari, E. *J. Catal.* **1985**, *92*, 340.

(32) Ng, K. Y. S.; Gulari, E. *J. Catal.* **1985**, *95*, 33.

(33) Van Veen, J. A. R.; Dewit, H.; Emeis, C. A.; Hendriks, R. A. J. M. *J. Catal.* **1987**, *107*, 579.

(34) Spanos, N.; Matralis, H. K.; Kordulis, Ch.; Lycourghiotis A. *J. Catal.* **1992**, *136*, 432.

(35) Bourikas, K.; Spanos, N.; Lycourghiotis A. *J. Colloid Interface Sci.* **1996**, *184*, 301.

(36) Perona, M. J.; Leckie, J. O. *J. Colloid Interface Sci.* **1985**, *106*, 64.

(37) Černic, M.; Borkovec, M.; Westall, J. C. *Langmuir* **1996**, *12*, 6127.

(38) Rietra, P. J. J.; Hiemstra, T.; Van Riemsdijk, W. H. *Geochim. Cosmochim. Acta* **1999**, *63*, 3009.

(39) Georgiadou, I.; Spanos, N.; Papadopoulou, Ch.; Matralis, H.; Kordulis, Ch.; Lycourghiotis A. *Colloids Surf. A* **1995**, *98*, 155.

(40) Spanos, N.; Georgiadou, I.; Lycourghiotis A. *J. Colloid Interface Sci.* **1995**, *172*, 374.

(41) Contescu, C.; Popa, V. T.; Schwarz, J. A. *J. Colloid Interface Sci.* **1996**, *180*, 149.

(42) Giacomelli, C.; Avena, M. J.; De Pauli C. P. *Langmuir* **1995**, *11*, 3483.

(43) Keizer, M. G.; Van Riemsdijk, W. H. *ECOSAT*: Technical Report of the Department of Soil Science and Plant Nutrition; Wageningen University: Wageningen, The Netherlands, 1998.

(44) Pauling, L. *J. Am. Chem. Soc.* **1929**, *51*, 1010.

(45) Hiemstra, T.; Van Riemsdijk, W. H.; Bolt, G. H. *J. Colloid Interface Sci.* **1989**, *133*, 91.

(46) Hiemstra, T.; De Wit, J. C. M.; Van Riemsdijk, W. H. *J. Colloid Interface Sci.* **1989**, *133*, 105.

(47) Hiemstra, T.; Venema, P.; Van Riemsdijk, W. H.; *J. Colloid Interface Sci.* **1996**, *184*, 680.

(48) Waychunas, G. A.; Rea, B. A.; Fuller, C. C.; Davis, J. A. *Geochim. Cosmochim. Acta* **1993**, *57*, 2251.

(49) Russel, J. D.; Parfitt, R. L.; Fraser, A. R.; Farmer, V. C. *Nature* **1974**, *248*, 220.

(50) Torrent, J.; Barrón, V.; Schwertmann, U. *Soil Sci. Soc. Am. J.* **1990**, *54*, 1007.

(51) Bargar, J. R.; Brown, G. E. Jr.; Parks, G. A. *Geochim. Cosmochim. Acta* **1997**, *61*, 2639.

(52) Yates, D. E.; Levine, S.; Healy, T. W. *J. Chem. Soc., Faraday Trans. 1* **1974**, *70*, 1807.

(53) Davis, J. A.; Leckie, J. O. *J. Colloid Interface Sci.* **1978**, *67*, 90.

(54) Hiemstra, T.; Van Riemsdijk, W. H. *Colloids Surf.* **1991**, *59*, 7.

(55) Baes, C. F., Jr.; Mesmer, R. E. *The Hydrolysis of Cations*; Wiley: New York, 1976.

(56) Pope, M. T. In *Encyclopedia of Inorganic Chemistry*; Bruce King, R., Ed.; Wiley: New York, 1994; Vol. 6.

(57) Lindqvist, I. *Ark. Kemi* **1951**, *2*, 325, 349.

(58) Smith, R. M.; Martell, A. E. *Critical Stability Constants*; Plenum: New York, 1981; Vol. 4.

(59) Spanos, N.; Vordonis, L.; Kordulis, Ch.; Lycourghiotis A. *J. Catal.* **1990**, *124*, 301.

(60) Kostov, I. In *Mineralogy*; Oliver and Boyd: Edinburgh, 1968.

(61) Parfitt, G. D. In *Progress in Surface and Membrane Science*; Cadenhead, D. A., Danielli, J. F., Eds.; Academic Press: New York, 1976; Vol. 11, p 181.

(62) Bourikas, K.; Hiemstra, T.; Van Riemsdijk, W. H., *Langmuir*, in press.

(63) Spanos, N.; Lycourghiotis A. *Langmuir* **1993**, *9*, 2250.

(64) Spanos, N.; Lycourghiotis A. *J. Colloid Interface Sci.* **1995**, *171*, 306.

(65) Gatehouse, B. M.; Leverett, P. *Chem. Commun.* **1968**, 901.

(66) Shimao, E. *Nature* **1967**, *214*, 170.